1-1-2020

Determination of demagnetizing factors using first-order reversal curves and ferromagnetic resonance

K. S. Muster
San Jose State University

R. Heindl
San Jose State University, ranko.heindl@sjsu.edu

Recommended Citation

K. S. Muster and R. Heindl. "Determination of demagnetizing factors using first-order reversal curves and ferromagnetic resonance" *AIP Advances* (2020). https://doi.org/10.1063/1.5129969

Determination of demagnetizing factors using first-order reversal curves and ferromagnetic resonance

Cite as: AIP Advances **10**, 015318 (2020); https://doi.org/10.1063/1.5129969
Submitted: 02 October 2019 • Accepted: 09 December 2019 • Published Online: 10 January 2020

K. S. Muster and R. Heindl

Determination of demagnetizing factors using first-order reversal curves and ferromagnetic resonance

Cite as: AIP Advances 10, 015318 (2020); doi: 10.1063/1.5129969
Presented: 5 November 2019 • Submitted: 2 October 2019 •
Accepted: 9 December 2019 • Published Online: 10 January 2020

K. S. Muster and R. Heindl[a)]

AFFILIATIONS

Department of Physics and Astronomy, San Jose State University, San Jose, California 95112, USA

Note: This paper was presented at the 64th Annual Conference on Magnetism and Magnetic Materials.
[a)]**Electronic mail:** ranko.heindl@sjsu.edu.

ABSTRACT

We present a method to quantitatively analyze magnetizing or demagnetizing interactions in arrayed nano-magnets by combining first-order reversal curve (FORC) and ferromagnetic resonance (FMR) measurement data. We develop a function to predict the resulting FORC distribution given: (1) a Gaussian intrinsic distribution in terms of the internal field and (2) a mean interaction field proportional to the sample's magnetic moment. We then perform least-squares regression of our model on experimental FORC measurements of a nanowire array and of a thin film. Combining the obtained interaction field with an FMR fit result allows us to algebraically solve for the effective axial and transverse demagnetizing factors. Our experimental demagnetizing factors agree with expected values and provide quantitative evidence of the demagnetizing interaction between nanowires in an array.

I. INTRODUCTION

Arrayed nano-magnets are useful media in memory devices for their magnetic reversal behavior,[1–3] an effect of the individual elements or the interactions between them.[4,5] Reversal can be characterized using first-order reversal curve (FORC) measurement, a technique used by multiple fields to study samples of many components or grains.[6–9] The FORC distribution is the calculated 2D map of reversal mechanisms, known as hysterons, that collectively model the sample's magnetic moment.[10,11]

Early studies of magnetic media have accounted for the observed FORC distribution shape by considering a mean internal interaction field.[12,13] Later studies have reproduced empirical FORC features by simulating FORC measurement of interacting hysterons[14] and arrays of idealized particles.[13,15,16] Then, interactions were successfully quantified from an experimental FORC distribution by comparison and fine-tuning of simulation parameters.[14,16] Other successful methods quantify interactions by characterizing the distribution shape while accounting for[17] or correcting for[18,19] interaction effects.

Like Gilbert *et al.*,[16] we extract quantitative information by comparing theoretical and experimental FORC diagram shapes. Rather than simulating the system, we present a function which directly predicts the theoretical FORC distribution in the presence of a mean interaction field. The function inputs describe the interaction field and the intrinsic, or operative, hysteron distribution from variables defined in Section IV. We then analyze an experimental FORC distribution by least-squares regression with our function, which quantifies the interaction and identifies the intrinsic distribution.

The interaction between parallel nanowires in an array is the internal demagnetizing field, H_d, from the dipole fields of nanowires magnetized axially.[14] The demagnetizing effect can be approximated using a mean negative interaction field, H_{int}.[16] Combining maximum H_d from FORC analysis with the effective magnetization, M_{eff}, from ferromagnetic resonance (FMR) provides the array's effective demagnetizing factors, $N = H_d/M$.[20] We present this method of combining FORC and FMR for characterizing magnetostatic interactions in arrayed nano-structures.

II. SAMPLE PREPARATION

Several nickel nanowire arrays with varying nanowire length and several thin nickel films of varying thickness have been prepared and analyzed. We expect these two structures to have large negative and near-zero interaction fields, respectively. Results of one nanowire array and one thin film are presented here, representing typical results.

The nanowire array sample is prepared by 2-probe electrodeposition into an alumina nanopore template, gold-plated on one side, made by InRedox.[21] Nickel is deposited using a 20 A/cm^2 DC current through a watts solution that is similar to that of Galicia-Aguilar *et al.*: 300 g/L $SiSO_4$, 60 g/L NiCl, 35 g/L H_3BO_3.[22] For grain refinement and better nanopore filling, 1.2 g/L soluble saccharin is added.[23] The template contains nanopores that are 80 nm in diameter and are close-packed with (11±2)% porosity. Average nanowire length is estimated to be (4.6±8) μm from measured saturation moment, template geometry, and the saturation magnetization of bulk nickel.[24]

The thin film is deposited onto a gold-covered glass substrate. Film thickness is estimated from measured saturation moment to be (184±2) nm.

III. MEASUREMENT

The array's axial magnetic moment, perpendicular to the sample plane, is measured by vibrating sample magnetometry. FORC measurements are performed by measuring magnetic moment, m, along ascending sweeps of applied field, H, from initial fields along the descending major curve, H_R. Each FORC is unique since it retains the magnetic memory of the initial magnetic state. We measure 118 such FORCs with 2×10^3A/m (2.5 mT) step size in H and H_R, shown in Fig. 1.

The FORC density at a point on the FORC diagram, (h_b, h_a), is calculated by the mixed derivative,[11]

$$m_s\,\rho(h_b, h_a) = -\frac{1}{2}\,\frac{\partial^2 m}{\partial H\,\partial H_R}. \tag{1}$$

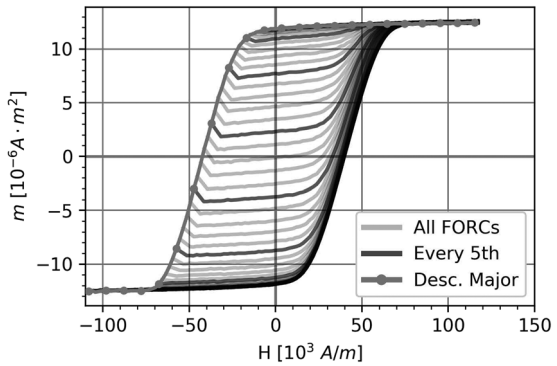

FIG. 1. The family of FORCs of the nanowire array sample is measured and used to calculate the FORC distribution. Magnetic moment, m, is measured while sweeping applied field, H, upward from initial fields along the descending major curve, H_R.

The resulting plot of ρ, known as the FORC distribution, maps the introduction of hysteresis, or irreversible change in moment, by the initial state. The FORC distribution and axes are formally defined in Section IV.

In a sample with strong interactions, reversal occurs relative to the total internal field instead of the applied external field.[12] The resulting experimental FORC distribution is a distorted representation of an intrinsic distribution.[12] Therefore, the experimental FORC distribution shape may be analyzed to quantify the interaction field in samples,[14,25] as we do in Section V.

The array's axial dynamic susceptibility is obtained by field-swept VNA FMR. An axial static field is swept downward from 715×10^3A/m (900 mT) to keep the sample saturated at $M = M_s$. The dynamic excitation is from microwaves with frequencies 10 - 18 GHz, supplied and measured by a vector network analyzer (VNA). Complex susceptibility is calculated from measured S-parameters after correcting for the contribution from the waveguide.[26,27] The complex susceptibility curve of each frequency value is fit to find the resonant field.

The resonance field versus frequency is then fit using the expected equation,

$$H_{\rm res}(\omega) = \frac{\omega}{\gamma\mu_0}\sqrt{1+\alpha^2} - (N_{\rm tr} - N_{\rm ax})M_s, \tag{2}$$

derived from the Landau-Lifshitz-Gilbert (LLG) equation,[28] where ω is the controlled microwave angular frequency, μ_0 is the permeability of free space, γ is the material's gyromagnetic ratio, M_s is the material's saturation magnetization, α is the sample's Gilbert damping constant, $N_{\rm ax}$ is the sample's demagnetizing factor in the axial direction of the nanowires, and $N_{\rm tr}$ is the sample's demagnetizing factor transverse to the nanowires. The y-intercept is related to the internal dynamic demagnetizing field. FMR fitting is traditionally used to experimentally obtain M_s while assuming ideal demagnetizing factors.[29] Instead, we are interested in the unknown demagnetizing field, which we consider in our model of FORC results.

IV. MODEL OF THE FORC DISTRIBUTION

The classic Preisach model describes a sample as a collection of elementary units called hysterons, described as binary hysteresis loops.[10] A hysteron is defined by its descending and ascending switching fields, h_a and h_b. For a system of N discrete hysterons, the sample's moment at any time is[11]

$$m(t) = \frac{m_s}{N}\sum_i^N \gamma_i(t), \tag{3}$$

where $\gamma_i = \pm1$ is the present state of the $i^{\rm th}$ hysteron depending on the magnetic history, $H(t)$. In the FORC measurement procedure, the hysteron states at applied fields, (H, H_R), are[11]

$$\gamma(h_b, h_a, H, H_R) = \begin{cases} -1 & H_R < h_a \text{ and } H < h_b, \\ +1 & \text{otherwise.} \end{cases} \tag{4}$$

In the case of a continuous distribution of hysterons,[11]

$$m(t) = m_s \iint \rho(h_b, h_a)\,\gamma(h_b, h_a, t)\,dh_b\,dh_a, \tag{5}$$

where ρ is the Preisach density, the relative contribution from a hysteron with particular switching fields. The FORC distribution is the experimental representation of the Preisach distribution of a measured sample. In real ferromagnetic samples with negligible inter-particle interactions, the Preisach distribution is typically a distribution of coercivity, h_c, satisfying $-h_a = h_b = h_c$.[12]

We employ the moving Preisach model in which reversal occurs relative to the internal (instead of applied) field, denoted $\widetilde{H}$. Hysterons have an intrinsic Preisach distribution, $\widetilde{\rho}(\widetilde{h}_b, \widetilde{h}_a)$, which is different from the observed FORC distribution, $\rho(h_b, h_a)$.[12] We model a Gaussian distribution of intrinsic coercivity, $\widetilde{h}_c = (\widetilde{h}_b - \widetilde{h}_a)/2$, as assumed by Gilbert *et al.*[16] The width in the perpendicular axis, $\widetilde{h}_u = (\widetilde{h}_b + \widetilde{h}_a)/2$, is included in the final evaluation but excluded in deriving the model to allow solving integrals from Eq. (5). The 2D intrinsic distribution, defined in Appendix, is determined by the function inputs: volume (scales amplitude), V; peak coordinates, $\widetilde{h}_{c,0}$ and $\widetilde{h}_{u,0}$; and widths, $\widetilde{\Delta}_c$ and $\widetilde{\Delta}_u$.

The interaction field allows transformation from the observed reversal fields, (h_b, h_a), to internal fields,[12]

$$\widetilde{h}_b(h_b, h_a) = h_b + H_{\text{int}}(h_b, h_a), \tag{6a}$$

$$\widetilde{h}_a(h_a) = h_a + H_{\text{int}}(h_a, h_a). \tag{6b}$$

We model a mean interaction field proportional to magnetic moment,

$$H_{\text{int}}(H, H_R) = k\,m = (k\,m_s)(m/m_s) = H_{\text{int,s}}\,r(H, H_R), \tag{7}$$

where k is the proportionality constant, $r(H, H_R)$ is the normalized magnetic moment, and $H_{\text{int,s}}$ is the interaction field at positive saturation, the maximum magnitude. The interaction field distorts the intrinsic Preisach distribution to form the observed FORC distribution.[12] We neglect the statistical interaction field[18] accounting for non-uniformity,[12] and edge effects.[30] In this study the negative interaction field represents the demagnetizing field at saturation,

$$H_{\text{int, s}} = -N_{\text{ax}} M_s, \tag{8}$$

where N_{ax} is the effective axial demagnetizing factor of the array.

We algebraically predict the resulting 1D distribution(s) of a narrow Gaussian distribution of intrinsic coercivity, $\widetilde{h}_c = (\widetilde{h}_b - \widetilde{h}_a)/2$, displaced by interactions according to Eqs. (6). The resulting distribution must yield self-consistent mean interaction fields by integration, Eq. (5). In the case of a demagnetizing interaction, we find two distinct, self-consistent 1D distributions defined in Appendix depending on the assumed sign of the resulting slope. We consider these to be analogous to the interaction field distribution (IFD) and coercive field distribution (CFD) typically observed in experimental FORC measurements of nanowire arrays.[31]

Our FORC function is the 2D distribution distorted by mean interaction fields calculated from the 1D solution. The 1D distribution is calculated directly from function inputs. The integral of the 1D distribution, Eq. (5), provides estimates for $r(h_b, h_a)$ at any point. Using the estimated interaction fields from Eqs. (6), the applied switching fields, (h_b, h_a), are transformed to intrinsic switching fields, $(\widetilde{h}_b, \widetilde{h}_a)$, by Eq. (7). The function output is the FORC density at a point on the input-defined intrinsic distribution, $\widetilde{\rho}(\widetilde{h}_b, \widetilde{h}_a)$. This algorithm is presented explicitly in Appendix. Different function inputs produce a variety of expected FORC distribution shapes, which match descriptions by Gilbert *et al.*[16]

V. DETERMINATION OF DEMAGNETIZING FACTORS

We use the model function, described in Section IV and defined in Appendix, to perform non-linear least-squares regression analysis on the experimental FORC distribution of each sample. The regression result is compared to the experimental FORC distribution of the nanowire array sample in Fig. 2.

The experimental CFD and IFD shapes match the model distribution's high density contour. Therefore, the experimental distribution shape can be attributed to a negative interaction field that distorts the intrinsic reversal fields of elements in the array. Minor discrepancies are apparent in the extent and sharpness of the low density contour.

The parameters obtained from regression are shown in Table I and represent the magnetic properties of elements in the array. The intrinsic distribution is mostly a distribution in $\widetilde{h}_c$, which represents hysterons with inversion-symmetry and verifies accuracy.[12,18] The distribution in $\widetilde{h}_u$ represents a component of interaction field that is not accounted for by the mean field, such as the interaction field variance mentioned in Section IV. Note that V is an amplitude scaling factor representing the intrinsic volume and not the model's resulting volume, found numerically to be (90±10)% of m_s, accounting for most of the change in m.

From FMR fitting, we obtain the effective magnetization term, $M_{\text{eff}} = (230\pm70)\times10^3$ A/m (290 mT). We observe that M_{eff} from FMR and $H_{\text{int,s}}$ from FORC both depend on the nanowire array's saturation magnetization and effective demagnetizing factors. We have the system of equations,

$$H_{\text{int, s}} = -N_{\text{ax}} M_s, \tag{9}$$

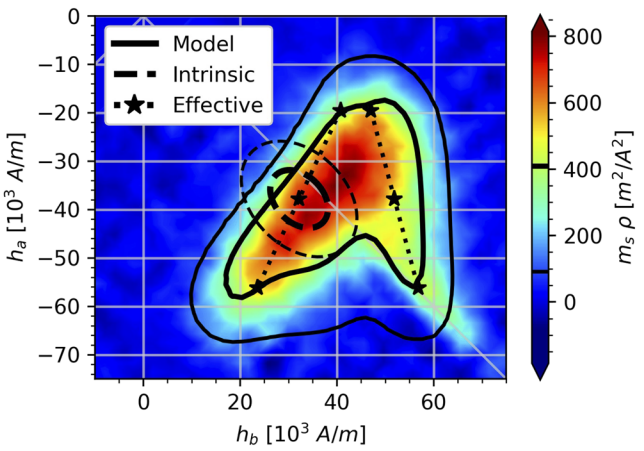

FIG. 2. Least-squares regression is performed on the experimental FORC distribution, $m_s\rho(h_b, h_a)$ (color scale), of a nanowire array using the model distribution (solid contours). The Gaussian intrinsic distribution of hysterons (dashed contours at 1 and 2 standard deviations) is distorted by the interaction field, estimated from a 1D solution (dotted with stars at the center and 1 standard deviation).

TABLE I. Nanowire array and thin film FORC regression results. See Appendix for variable definitions and the regression function.

Variable	Nanowire array [10^3A/m]	Thin film [10^3A/m]
$H_{\text{int,s}}$	−20 ± 2	+0.38 ± 0.09
$\widetilde{h}_{c,0}$	35.0 ± 0.6	5.15 ± 0.04
$\widetilde{\Delta}_c$	4.9 ± 0.5	0.99 ± 0.03
$\widetilde{h}_{u,0}$	−3 ± 1	−0.09 ± 0.03
$\widetilde{\Delta}_u$	3.4 ± 0.7	0.54 ± 0.02
V/m_s [%]	7 ± 1	47 ± 3

$$M_{\text{eff}} = M_s(N_{\text{tr}} - N_{\text{ax}}), \tag{10}$$

$$1 = N_{\text{ax}} + N_{\text{tr}} + N_{\text{tr}}, \tag{11}$$

the third equation being a general property of demagnetizing factors along principle axes.[32] We solve for the three unknown quantities,

$$M_s = (500 \pm 200) \times 10^3 \text{A/m}, \tag{12a}$$

$$N_{\text{ax}} = (3.8 \pm 11) \times 10^{-3}, \tag{12b}$$

$$N_{\text{tr}} = (4.81 \pm 5) \times 10^{-3}. \tag{12c}$$

Combining analysis from FORC and FMR provides the effective demagnetizing factors of the array.

The experimental value for N_{ax} can be compared to the expected values for simple geometries. An isolated nanowire has $N_{\text{ax}} = 0$ when assuming infinite length, or $N_{\text{ax}} = 1.1 \times 10^{-3}$ when considering our nanowires' aspect ratio.[32] The observed value is too large to represent that of an isolated nanowire, so it must also depend on the array geometry. In Fig. 3, we illustrate the limit of decreasing nanowire spacing until the sample forms an infinite continuous film, in which case $N_{\text{ax}} \to 1$.[20] Functions developed by

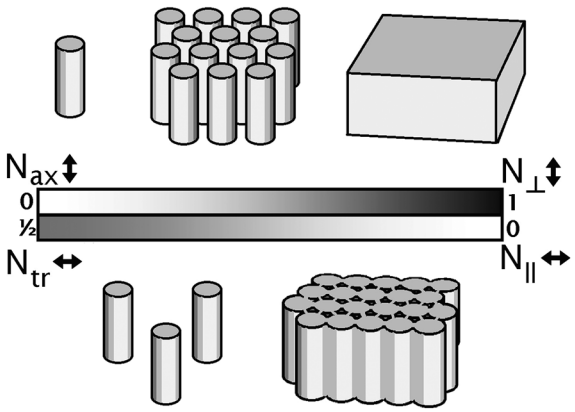

FIG. 3. The demagnetizing factors in the axial direction, N_{ax}, and transverse direction, N_{tr}, are expected to depend on nanowire spacing. The limiting cases are the isolated nanowire and the continuous slab.

Clime *et al.* from simulated nanowire arrays yield the demagnetizing field as a function of array geometry, yielding $N_{\text{ax}} = (80 \pm 20) \times 10^{-3}$ for our sample.[20] This matches the order of magnitude of our result. Under-valued interaction strength could be attributed to our model's low-density contours under-valuing CFD length or neglecting the interaction strength variance.

Least squares regression of the thin film FORC data in Table I shows that the FORC distribution shape can be accounted for by a positive mean interaction, negligable in magnitude compared to the bulk magnetization of nickel. A past simulation of non-interacting particles following the Stoner-Wohlfarth model has resulted in a similar FORC distribution shape.[14] The thin film FMR fit includes a relevant quantity similar to that of the nanowire array, $M_{\text{eff}} = M_s(N_\perp - N_\parallel)$. The combined results from FORC and FMR are

$$M_s = (420 \pm 110) \times 10^3 \text{A/m}, \tag{13a}$$

$$N_\parallel = (-900 \pm 300) \times 10^{-6}, \tag{13b}$$

$$N_\perp = 1.0018 \pm 0.0006. \tag{13c}$$

The experimental demagnetizing factors are close to those of the ideal infinite plane,[29] and the value of saturation magnetization is reasonable.[24] This verifies the accuracy of our model in the absence of mean field interactions, in which case the observed FORC distribution represents intrinsic reversal fields.

VI. CONCLUSION

We have developed a function that models a general observed FORC distribution in a sample with strong demagnetizing field. Least-squares regression has allowed extracting quantitative information from an experimental FORC distribution, including the mean demagnetizing field strength in saturation. We believe this quantity represents the mean dipole field in the sample from neighboring nanowires.

By combining FORC results with FMR results, we have determined the effective demagnetizing factors of the array and the thin film. The array's experimental axial demagnetizing factor is an order of magnitude larger that of a theoretical isolated nanowire, an expected effect of finite nanowire spacing. Our method for obtaining the demagnetizing factors of a sample by combined FORC and FMR results allows quantifying interactions within an arrayed sample.

APPENDIX: FORC FUNCTION

Here we present the algorithm of our 2D FORC function used in least-squares regression. Our function models FORC density, ρ, at a point on the FORC diagram representing hysterons with applied switching fields, (h_b, h_a). The other function inputs describe the intrinsic distribution of hysteron switching fields and the interaction field with a maximum value of $H_{\text{int,s}}$. The intrinsic distribution is a 2D Gaussian defined in the internal field basis, $(\widetilde{h}_c, \widetilde{h}_u)$ by: its volume, V (an amplitude scaling factor); peak position, $(\widetilde{h}_{c,0}, \widetilde{h}_{u,0})$; and single standard deviation widths, $\widetilde{\Delta}_c$ and $\widetilde{\Delta}_u$.

Finding the internal fields requires integration over the resulting distribution, which we first approximate with a narrow, tilted, 1D Gaussian distribution. For systems with magnetizing interactions, specifically $H_{\text{int, s}} > -\widetilde{\Delta}_c$, the 1D distribution is described by the IFD

with derived position,

$$h_{a,0} = \widetilde{h}_{u,0} - \widetilde{h}_{c,0}, \tag{A1a}$$

$$h_{b,0}^{\mathrm{IFD}} = \widetilde{h}_{u,0} + \widetilde{h}_{c,0}. \tag{A1b}$$

Width and tilt are defined by components of the vector, (Δ_b, Δ_a), from the center to one standard deviation away,

$$\Delta_a = \widetilde{\Delta}_c - H_{\mathrm{int,s}}\,\mathrm{erf}\left(1/\sqrt{2}\right), \tag{A1c}$$

$$\Delta_b^{\mathrm{IFD}} = -\widetilde{\Delta}_c - H_{\mathrm{int,s}}\,\mathrm{erf}\left(1/\sqrt{2}\right). \tag{A1d}$$

In systems with strong demagnetizing interactions, the CFD may also be present. The CFD has the same h_a projection as the IFD. The CFD position and width in h_b are

$$h_{b,0}^{\mathrm{CFD}} = \widetilde{h}_{u,0} + \widetilde{h}_{c,0} - H_{\mathrm{int,s}}\,\mathrm{erf}\left(1/\sqrt{2}\right), \tag{A1e}$$

$$\Delta_b^{\mathrm{CFD}} = \widetilde{\Delta}_c. \tag{A1f}$$

The IFD and CFD positions and widths agree with descriptions by previous simulation studies.[16,17]

The integral over the distribution with respect to h_a using using Eq. (5) predicts the descending major curve's normalized moment at any descending field from saturation, H_R. The result from the distribution defined by Eq. (A1a) and Eq. (A1c) is

$$r_{\downarrow}(H_R) = \mathrm{erf}\left(\frac{H_R - h_{a,0}}{\Delta_a\sqrt{2}}\right). \tag{A2a}$$

The ascending minor curve's normalized moment is $r_{\uparrow}(H, H_R) = [r_{\uparrow}^{\mathrm{IFD}} + r_{\uparrow}^{\mathrm{CFD}}]/2$ for demagnetizing interactions and $r_{\uparrow}(H, H_R) = r_{\uparrow}^{\mathrm{CFD}}$ for magnetizing. These terms are calculated for the distribution defined by Eqs. (A1) also using Eq. (5) and the regions of state from Eq. (4), giving

$$r_{\uparrow}^{\mathrm{IFD}} = \max\left\{r_{\downarrow}(H_R),\ \mathrm{erf}\left(\frac{H - h_{b,0}^{\mathrm{IFD}}}{\Delta_b^{\mathrm{IFD}}\sqrt{2}}\right)\right\}, \tag{A2b}$$

$$r_{\uparrow}^{\mathrm{CFD}} = \min\left\{1,\ 1 + r_{\downarrow}(H_R) + \mathrm{erf}\left(\frac{H - h_{b,0}^{\mathrm{CFD}}}{\Delta_b^{\mathrm{CFD}}\sqrt{2}}\right)\right\}. \tag{A2c}$$

The normalized moments allow solving for internal fields,[12]

$$\widetilde{h}_a = h_a - H_{\mathrm{int,s}} r_{\downarrow}(h_a), \tag{A3a}$$

$$\widetilde{h}_b = h_b - H_{\mathrm{int,s}} r_{\uparrow}(h_b, h_a). \tag{A3b}$$

These are converted to the $(\widetilde{h}_c, \widetilde{h}_u)$ basis of the intrinsic distribution,

$$\widetilde{h}_c = (\widetilde{h}_b - \widetilde{h}_a)/2, \tag{A4a}$$

$$\widetilde{h}_u = (\widetilde{h}_b + \widetilde{h}_a)/2. \tag{A4b}$$

Lastly, the observed density, ρ, is considered to be equal to the intrinsic density $\widetilde{\rho}$ at the field values from Eqs. (A4). The 2D Gaussian intrinsic distribution is defined using function inputs,

$$\tilde{\rho} = \frac{V}{2\widetilde{\Delta}_c\widetilde{\Delta}_u}\exp\left[-\left(\frac{\widetilde{h}_c - \widetilde{h}_{c,0}}{\sqrt{2}\,\widetilde{\Delta}_c}\right)^2 - \left(\frac{\widetilde{h}_u - \widetilde{h}_{u,0}}{\sqrt{2}\,\widetilde{\Delta}_u}\right)^2\right]. \tag{A5}$$

The function output is the resulting density at a position on the FORC distribution, $\rho(h_b, h_a)$, given a particular intrinsic distribution, $\widetilde{\rho}(\widetilde{h}_c, \widetilde{h}_u)$, and magnetizing or demagnetizing interaction strength, $H_{\mathrm{int,s}}$.

REFERENCES

[1] C. J. O'Connor, "Survey of recent developments in the synthesis, structure, and physical properties of nanostructured magnetic materials," Tech. Rep. (University of New Orleans and Army Research Office, 1996).
[2] C. Ross, "Patterned magnetic recording media," Annu. Rev. Mater. Res **31**, 203–235 (2001).
[3] B. Engel, J. Akerman, B. Butcher, R. Dave, M. DeHerrera, M. Durlam, G. Grynkewich, J. Janesky, S. Pietambaram, N. Rizzo *et al.*, "A 4-Mb toggle MRAM based on a novel bit and switching method," IEEE Trans. Magn **41**, 132–136 (2005).
[4] T. Aign, P. Meyer, S. Lemerle, J. Jamet, J. Ferré, V. Mathet, C. Chappert, J. Gierak, C. Vieu, F. Rousseaux *et al.*, "Magnetization reversal in arrays of perpendicularly magnetized ultrathin dots coupled by dipolar interaction," Phys. Rev. Lett **81**, 5656 (1998).
[5] X. Kou, X. Fan, R. K. Dumas, Q. Lu, Y. Zhang, H. Zhu, X. Zhang, K. Liu, and J. Q. Xiao, "Memory effect in magnetic nanowire arrays," Adv. Mater **23**, 1393–1397 (2011).
[6] T. Zelinka, P. Hejda, and V. Kropáček, "The vibrating-sample magnetometer and Preisach diagram," Phys. Earth Planet. Inter **46**, 241–246 (1987).
[7] C. R. Pike, A. P. Roberts, and K. L. Verosub, "Characterizing interactions in fine magnetic particle systems using first order reversal curves," J. Appl. Phys **85**, 6660–6667 (1999).
[8] T. Schrefl, T. Shoji, M. Winklhofer, H. Oezelt, M. Yano, and G. Zimanyi, "First order reversal curve studies of permanent magnets," J. Appl. Phys **111**, 07A728 (2012).
[9] V. Franco, F. Béron, K. Pirota, M. Knobel, and M. Willard, "Characterization of the magnetic interactions of multiphase magnetocaloric materials using first-order reversal curve analysis," J. Appl. Phys **117**, 17C124 (2015).
[10] F. Preisach, "Uber die magnetische nachwirkung," Z. Phys **94**, 277–302 (1935).
[11] I. D. Mayergoyz, "Mathematical models of hysteresis," Phys. Rev. Lett **56**, 1518–1521 (1986).
[12] E. Della Torre, "Effect of interaction on the magnetization of single-domain particles," IEEE Trans. Audio Electroacoust **14**, 86–92 (1966).
[13] A. Stancu, C. Pike, L. Stoleriu, P. Postolache, and D. Cimpoesu, "Micromagnetic and Preisach analysis of the first order reversal curves (FORC) diagram," J. Appl. Phys **93**, 6620–6622 (2003).
[14] C. R. Pike, C. A. Ross, R. T. Scalettar, and G. Zimanyi, "First-order reversal curve diagram analysis of a perpendicular nickel nanopillar array," Phys. Rev. B **71**, 134407 (2005).
[15] A. Muxworthy, D. Heslop, and W. Williams, "Influence of magnetostatic interactions on first-order-reversal-curve (FORC) diagrams: A micromagnetic approach," Geophys. J. Int **158**, 888–897 (2004).
[16] D. A. Gilbert, G. T. Zimanyi, R. K. Dumas, M. Winklhofer, A. Gomez, N. Eibagi, J. L. Vicent, and K. Liu, "Quantitative decoding of interactions in tunable nanomagnet arrays using first order reversal curves," Sci. Rep **4**, 4204 (2014).
[17] F. Béron, L. Clime, M. Ciureanu, D. Ménard, R. W. Cochrane, and A. Yelon, "Magnetostatic interactions and coercivities of ferromagnetic soft nanowires in uniform length arrays," J. Nanosci. Nanotechnol **8**, 2944–2954 (2008).
[18] P. Postolache, M. Cerchez, L. Stoleriu, and A. Stancu, "Experimental evaluation of the Preisach distribution for magnetic recording media," IEEE Trans. Magn **39**, 2531–2533 (2003).
[19] R. Tanasa and A. Stancu, "Statistical characterization of the FORC diagram," IEEE Trans. Magn **42**, 3246–3248 (2006).
[20] L. Clime, F. Béron, P. Ciureanu, M. Ciureanu, R. Cochrane, and A. Yelon, "Characterization of individual ferromagnetic nanowires by in-plane magnetic measurements of arrays," J. Magn. Magn. Mater **299**, 487–491 (2006).
[21] InRedox, AAO Wafers with Metal Contacts, https://www.inredox.com/product/aao-wafers-contact/.

[22]G. Galicia-Aguilar, G. Campo-García, J. Ramírez-Reyes, and A. Medina-Almazán, "Study of the magnetic field effect on the electrochemical behavior of a nickel electrodeposit," Int. J. Electrochem. Sci **12**, 928–942 (2016).
[23]M. Bhardwaj, K. Balani, R. Balasubramaniam, S. Pandey, and A. Agarwal, "Effect of current density and grain refining agents on pulsed electrodeposition of nanocrystalline nickel," Surf. Eng **27**, 642–648 (2011).
[24]H. Danan, A. Herr, and A. J. P. Meyer, "New determination of the saturation magnetization of nickel and iron," J. Appl. Phys **39**, 669–670 (1968).
[25]S. Alikhanzadeh-Arani, M. Almasi-Kashi, and A. Ramazani, "Magnetic characterization of FeCo nanowire arrays by first-order reversal curves," Curr. Appl. Phys **13**, 664–669 (2013).
[26]Y. Ding, T. J. Klemmer, and T. M. Crawford, "A coplanar waveguide permeameter for studying high-frequency properties of soft magnetic materials," J. Appl. Phys **96**, 2969–2972 (2004).
[27]B. Buford, P. Dhagat, and A. Jander, "A technique for error estimation of linewidth and damping parameters extracted from ferromagnetic resonance measurements," J. Appl. Phys **117**, 17E109 (2015).
[28]T. L. Gilbert, "A phenomenological theory of damping in ferromagnetic materials," IEEE Trans. Magn **40**, 3443–3449 (2004).
[29]C. Kittel, "On the theory of ferromagnetic resonance absorption," Phys. Rev **73**, 155–161 (1948).
[30]C.-I. Dobrotă and A. Stancu, "Tracking the individual magnetic wires' switchings in ferromagnetic nanowire arrays using the first-order reversal curves (FORC) diagram method," Physica B: Condensed Matter **457**, 280–286 (2015).
[31]C.-I. Dobrotă and A. Stancu, "What does a first-order reversal curve diagram really mean? A study case: Array of ferromagnetic nanowires," J. Appl. Phys **113**, 043928 (2013).
[32]A. P. Guimarães, *Principles of Nanomagnetism*, Vol. 7 (Springer, 2009).